

IMPERIAL/TP/94-95/18
 CWRU-P2-1995
 NI94043
 hep-ph/9503223

Defect Production in Slow First Order Phase Transitions

Julian Borrill and T.W.B. Kibble

*Blackett Laboratory, Imperial College, London SW7 2BZ, United Kingdom and
 Isaac Newton Institute for Mathematical Sciences, Cambridge CB3 0EH, United Kingdom*

Tanmay Vachaspati

*Department of Physics, Case Western Reserve University
 10900 Euclid Ave., Cleveland OH 44106-7079, and
 Isaac Newton Institute for Mathematical Sciences, Cambridge CB3 0EH, United Kingdom*

Alexander Vilenkin

*Institute of Cosmology, Department of Physics and Astronomy,
 Tufts University, Medford MA 02155, USA and
 Isaac Newton Institute for Mathematical Sciences, Cambridge CB3 0EH, United Kingdom*
 (May 9, 2018)

Abstract

We study the formation of vortices in a U(1) gauge theory following a first-order transition proceeding by bubble nucleation, in particular the effect of a low velocity of expansion of the bubble walls. To do this, we use a two-dimensional model in which bubbles are nucleated at random points in a plane and at random times and then expand at some velocity $v_b < c$. Within each bubble, the phase angle is assigned one of three discrete values. When bubbles collide, magnetic ‘fluxons’ appear: if the phases are different, a fluxon–anti-fluxon pair is formed. These fluxons are eventually trapped in three-bubble collisions when they may annihilate or form quantized vortices. We study in particular the effect of changing the bubble expansion speed on the vortex density and the extent of vortex–anti-vortex correlation.

98.80.Cq, 11.17.+y

Typeset using REVTeX

I. INTRODUCTION

Cosmic strings are topological defects which may have been formed at a high-temperature phase transition very early in the history of the Universe [1]. To estimate their observational consequences, we need to follow the evolution of a network of cosmic strings, either analytically or numerically. In either case the starting point must be some estimate of the initial string density shortly after the symmetry-breaking phase transition. There has recently been considerable debate about this question, particularly in the case of gauge theories [2,3].

To be specific, we consider a spontaneously broken Abelian U(1) gauge theory, with a complex scalar field ϕ . At zero temperature, there is a degenerate ground state in which ϕ has a vacuum expectation value of fixed magnitude, but arbitrary phase. The symmetry is restored above some critical temperature T_c . The conventional picture of defect formation is this [4]: as the Universe cools, the phases in sufficiently far-separated regions are uncorrelated; if the phase change around a large loop in space is a non-zero multiple of 2π , then a string or strings must pass through it. If the transition is second-order, we may model the effect by considering the space as made up (at some temperature slightly below T_c) of separate domains whose size is determined by the length scales of the microphysics [5], and supposing that within each domain the phase is chosen randomly and independently. Across the boundary between two neighboring domains, the phase is assumed to interpolate smoothly between the two values, along the shortest path (this is called the ‘geodesic rule’) [6]. On the line where three domains meet, a string is trapped if the net phase change around the line is $\pm 2\pi$.

Here, we shall be particularly concerned with the case where the transition is *first-order*, proceeding by bubble nucleation. In this case, the expanding Universe supercools, remaining in the symmetric phase below the critical temperature. When it has cooled sufficiently, bubbles of the true-vacuum phase begin to nucleate and expand until they eventually percolate and fill the whole of space. We may then reasonably assume that the phase within each bubble is chosen randomly and independently.

There is of course a complication here, emphasized in a recent paper by Rudaz and Srivastava [2]: because of the gauge invariance, the phase of the field is not well-defined. Indeed unless we have fixed the gauge, even the *relative* phase between different bubbles is not meaningful. Is it then correct, in order to estimate the initial string density, to use a model in which a phase is randomly assigned in each bubble and strings are trapped when three bubbles meet if the net phase change is $\pm 2\pi$?

In a previous paper [7], two of us have analyzed the meaning of relative phase and the process of phase equilibration in a bubble collision. The relative phase can be given a gauge-invariant definition, in terms of the line integral of the covariant derivative. In general, that definition is path-dependent, but the *initial* phase difference is unambiguous, provided we may assume that the electromagnetic field is initially zero. We showed that, in the usually considered case where the bubble walls expand almost at the speed of light, phase equilibration always proceeds more slowly than bubble expansion, so that the simple model just described is indeed correct. However, this leaves open the question of what happens when the bubble walls expand more slowly, due to the damping effect of the ambient plasma. This is the question we aim to address in the present paper.

When two bubbles with different phases meet, a current flows across the interface. The

phase difference between the two bubbles (along their line of centres) oscillates with frequency determined by the gauge-field mass and decays due to damping by the plasma [7]. The current in turn generates a loop of magnetic flux surrounding the collision region. When the bubbles expand at close to the speed of light, the radius of the collision region, and hence of the flux loop, expands faster than c . (In that case, it is best to think of the flux not as expanding but as being created and decaying at successively larger radii.) Where three bubbles meet, the fluxes in the three separate loops combine. Of course the total flux trapped is then either zero or \pm a flux quantum. Because the flux is always tied to the collision region, we can find out whether a string is trapped merely by examining the initial phases of the three bubbles.

The situation is very different, however, if the bubble walls expand more slowly. Then the rate of expansion of the flux loop may be *less* than c , in which case it is quite possible that it might propagate away from the collision region and become separated from the bubbles that gave it birth. If that happens, it would be likely to suppress the number of strings produced and to affect their distribution — in particular the relative proportions of long strings and loops. One might think that if strings become rare, then most of them would be in the form of small closed loops [8]. If so, that would have a dramatic impact on cosmology.

The actual speed of magnetic flux spreading depends on the plasma conductivity in the region between the bubbles. A realistic simulation of all the processes involved would be very complicated, and we shall not attempt it here. Instead, we shall study a simple two-dimensional model and represent the flux spreading by the propagation of particle-like ‘fluxons’. Although it is obviously unrealistic in details, we believe that this model includes the essential features necessary to answer (qualitatively) our central question: what is the effect of flux spreading on the defect statistics?

We shall consider a two-dimensional space, in which circular bubbles nucleate at random and expand with some velocity v_b , and in which vortices may be trapped at the points where bubbles finally coalesce. When two bubbles meet, they generate not a loop of flux but a fluxon–anti-fluxon pair. For simplicity, we approximate the $U(1)$ phase angles by three discrete values ($0, \pm 2\pi/3$). Then all the fluxons generated carry the same flux (up to a sign). In units of the flux quantum, $2\pi/e$, the possible fluxon charges are $\pm 1/3$.

We assume that so long as the junction points of the colliding bubble walls move faster than certain critical speed $v_f > v_b$, the fluxons are fixed to them, but when the junction speed falls below v_f , the fluxons are freed and continue to move independently with speed v_f , bouncing off any other bubbles they encounter.

If we wait long enough of course the bubbles will percolate and fill the whole of space, so all fluxons will eventually become trapped. The gaps between the bubbles will finally close, trapping vortices with quantized flux, so the fluxons will either annihilate or be forced together in threes to form vortices. But of course the total flux trapped where three bubbles finally coalesce *cannot* now be found just by looking at their initial phases. Some of their fluxons may have escaped, while others from farther afield may have wandered in.

When a fluxon passes between two bubbles, it changes the relative phase between them. So to follow all the changes in phase as the system evolves would be a very complicated task. Fortunately, it is not necessary to do so. Our strategy will be not to choose the phases until it is necessary to do so, at bubble collisions. When two bubbles collide, there are two distinct cases. If they belong to *disjoint* bubble clusters, the relative phase between these clusters

has not yet been fixed, so we make a random choice, here restricted to the three discrete values. In principle it would be possible to trace the evolution of the phase difference back, following the movements of all the intervening fluxons, to discover what the initial phase difference was when the bubbles nucleated, but this is not something we ever need to know. Whenever it is chosen, the phase difference is random.

The other possibility is that the two bubbles belong to the *same* cluster. Then the collision completes a circuit within the bubble cluster, usually enclosing a region of the symmetric phase, or splitting an already enclosed region into two. (Other cases are described below.) In that case, the relative phase between the two colliding bubbles is already in principle fixed by earlier choices, so we do not have a random choice to make. In fact, by consistency, the relative phase must be such as to ensure that the total flux within the newly enclosed region is an integer number of flux quanta, i.e., that the net fluxon number is a multiple of three. In line with the geodesic rule, we assume the phase difference is as small as possible consistent with this condition. In other words, we create at most a single fluxon–anti-fluxon pair.

The algorithm we adopt is described in the following Section, its implementation in Section III and the results in Section IV. We are particularly interested in examining the dependence of the defect density on the velocity ratio v_b/v_f . If the bubble-wall velocity is low, one expects the number of defects per bubble to be reduced. This is because three-bubble collisions will less often trap strings, since the phases of the first two bubbles may have equilibrated before they encounter the third. In our model this effect is represented by the escape of the relevant fluxons. In the three-dimensional case, another effect could be to change the ratio of long strings to small loops. In two dimensions, the analogue of a small loop is a close vortex–anti-vortex pair, so we also study the ratio between the mean nearest-neighbor vortex–anti-vortex distance and the corresponding vortex–vortex one. For $v_b = v_f$, there is strong vortex–anti-vortex correlation: the ratio is substantially less than one. But for $v_b < v_f$ we shall see that, in contrast to models with tilted potentials [8], the reduction in the number of defects is accompanied by a *reduced* vortex–anti-vortex correlation. Our conclusions are discussed in Section V.

II. ALGORITHM

In the standard numerical simulations of defect production [6] relative phases are assigned at random to sites on a lattice corresponding to the centres of causally disconnected regions of true vacuum (either bubbles in a first-order or domains in a second-order transition). Between these sites the phase is taken to vary along the shortest path on the vacuum manifold — the so-called geodesic rule. Defects are then formed wherever this geodesic interpolation between sites generates a topologically nontrivial path in the vacuum manifold.

For a first-order transition this formalism corresponds to true vacuum bubbles nucleating simultaneously, equidistant from all their nearest neighbors. Consequently all collisions between neighboring bubbles occur simultaneously, and the associated phase differences are simply given by the differences in the initial assigned phases. In this paper we refine this approach in two ways. Firstly the bubbles are nucleated at random times and places, so that their collisions are also randomly distributed in time and space. Secondly, we consider

the effect of flux spreading on defect formation, with flux spreading being represented by the propagation of fluxons.

Our algorithm is therefore as follows:

1. generate a population of bubble nucleation events distributed randomly within some finite volume of 2+1 dimensional spacetime.
2. expand these bubbles at some fixed sub-luminal speed v_b .
3. at every 2-bubble collision determine the relative phase difference:–
 - (a) if the collision does not close off a region of false vacuum, assign the fluxon pair at the two intersection points at random.
 - (b) if the collision does close off a region of false vacuum, assign the fluxon pair at the two intersection points so as to round the total charge within the closed region to the nearest integer.
4. at every intersection point, determine the time at which the associated fluxon escapes, and follow its subsequent free evolution, bouncing it off any bubble that it encounters.
5. at every 3-bubble collision, sum the fluxons associated with the three intersections to give the total defect charge.

All the defects in this approach are ultimately formed at 3-bubble collisions (or equivalently at the collision of three two-bubble intersection points). However three bubbles can collide in two ways. In the first case (Fig. 1, called an external collision) all the collisions occur in the false vacuum and a closed curvilinear ‘triangle’ of false vacuum is formed whose vertices are the three two-bubble intersection points. As the bubbles expand this triangle shrinks to a point, condensing all the charge (both at the intersection points and in the form of free fluxons trapped in the closed region) into an integer-charged defect. This is the usual defect generating mechanism, and the only one available in lattice-based simulations. Alternatively (Fig. 2, called an internal collision) one of the three collisions occurs within the third bubble. In this case the three intersection points meet as the internal one emerges into the false vacuum. Although there is no closed region of false vacuum, if the two external intersection points carry fluxons of the same sign, this configuration generates a defect and an anti-fluxon. This can be viewed as the production of a virtual fluxon–anti-fluxon pair as the 1-2 intersection point emerges from bubble 3. The fluxon then joins with the 1-3 and 2-3 fluxons to generate a defect and the anti-fluxon is released. In the case of relativistic bubbles, it can be shown that the division of collisions into internal and external is frame-dependent. For any internal collision one can find a frame of reference where it is seen as external, and vice versa. Since defect production should be frame-independent, this suggests that the same rules should be applied to both types of collisions.

In our algorithm, the defects are held stationary once they are formed and we have ignored any evolution of the defect gas during the course of the phase transition. For the specific case we have in mind — the breaking of a $U(1)$ gauge symmetry in two dimensions — there are no long-range inter-defect forces and the only evolutionary effect would be due to the initial random velocities of the defects. Evolution due to such random velocities

would result in some mixing of the defects and will somewhat decrease the correlations of defect and anti-defect locations. In the case where there are long range inter-defect forces or in the case of strings in three dimensions where the string tension can be the cause of evolution, our results should be used with care. However, even in these cases, if the mean distance traversed by defects during the course of the phase transition is not larger than the inter-defect separation, our results would be applicable.

III. IMPLEMENTATION

Our simulation is sufficiently simple that it does not require discretization of space and time: the bubbles and fluxons can be evolved completely analytically. This, however, makes the implementation quite complicated. We have first to generate a population of bubbles, then to calculate when all the key events (2-bubble collision, fluxon freeing, and 3-bubble collision) occur, then to time-order these, and only then to work through including them in the simulation.

A. Preparation

To generate a population of bubbles we choose some predetermined number of random events, each lying within the designated simulation volume. Time-ordering these we reject all those which would correspond to a bubble being nucleated within another bubble. Finally we check *post hoc* that the remaining bubbles completely fill the simulation space by the end of the simulation time. We now have a time-ordered list of bubbles defined by their nucleation events

$$B_i \equiv (t_i, \mathbf{x}_i). \quad (1)$$

Next, we determine the coordinates of the collision event of every pair of bubbles. Any time-ordered pair B_i, B_j collide at $C_{ij} \equiv (t_{ij}, \mathbf{x}_{ij})$ when

$$r_i(t_{ij}) + r_j(t_{ij}) = |\Delta \mathbf{x}_{ij}|, \quad (2)$$

where $r_i = v_b(t - t_i)$ is the radius of bubble B_i expanding at speed v_b , and the spatial separation of the bubble centres is $\Delta \mathbf{x}_{ij} = \mathbf{x}_j - \mathbf{x}_i$. Solving for t_{ij} we find

$$t_{ij} = \frac{|\Delta \mathbf{x}_{ij}| + v_b(t_i + t_j)}{2v_b}. \quad (3)$$

The co-ordinates of the intersection points associated with collision C_{ij} at any time $t \geq t_{ij}$ are given by (Fig. 3)

$$\mathbf{x}_{ij}(t) = \mathbf{x}_i + \alpha(t)\hat{\mathbf{n}}_{ij} \pm \beta(t)\hat{\mathbf{n}}_{ij}^\perp, \quad (4)$$

where $\hat{\mathbf{n}}_{ij}$ is the unit vector along the line of centres from B_i to B_j , $\hat{\mathbf{n}}_{ij}^\perp$ is a unit vector perpendicular to $\hat{\mathbf{n}}_{ij}$, and

$$\alpha(t) = \frac{\Delta \mathbf{x}_{ij}^2 + r_i^2(t) - r_j^2(t)}{2|\Delta \mathbf{x}_{ij}|},$$

$$\beta(t) = \sqrt{r_i^2(t) - \alpha^2(t)}. \quad (5)$$

Calculating $\mathbf{x}_{ij}(t_{ij})$ and neglecting any collision occurring outside the simulation volume, all the remaining 2-bubble collision events are held in a time-ordered list.

Any fluxon associated with either of the above intersection points will be released when their speed falls below that of a free fluxon, v_f . Differentiating equation (4) with respect to time gives

$$\mathbf{v}_{ij}(t) = \dot{\alpha}(t)\hat{\mathbf{n}}_{ij} \pm \dot{\beta}(t)\hat{\mathbf{n}}_{ij}^\perp, \quad (6)$$

so the intersection points fall below the fluxon speed when

$$|\mathbf{v}_{ij}(t)| = v_f. \quad (7)$$

Solving for t we find

$$t = t_i + \frac{R_+}{v_b}, \quad (8)$$

where R_+ is the positive root of the equation

$$R^2 - v_b \Delta t_{ij} R + \frac{v_f^2(v_b^2 \Delta t_{ij}^2 - \Delta \mathbf{x}_{ij}^2)}{4(v_f^2 - v_b^2)} = 0, \quad (9)$$

and the temporal separation of the bubbles is $\Delta t_{ji} = t_j - t_i$. The location of the intersection points at this time are then given by equation (4). If such a point lies within another bubble at this time then any associated fluxon will already have been involved in a 3-bubble, defect-forming, collision and can be neglected. Again neglecting any events occurring outside the simulation volume the remaining potential fluxon-release events are also held in a time-ordered list.

Ultimately we want the coordinates of all 3-bubble collisions. In practice we only need consider time-ordered triplets B_i, B_j, B_k for which C_{ij}, C_{jk} and C_{ki} occur within the simulation time. Such a triplet collides at $D_{ijk} \equiv (t_{ijk}, \mathbf{x}_{ijk})$ when

$$\begin{aligned} |\mathbf{x}_{ijk} - \mathbf{x}_i| &= r_i(t_{ijk}), \\ |\mathbf{x}_{ijk} - \mathbf{x}_j| &= r_j(t_{ijk}), \\ |\mathbf{x}_{ijk} - \mathbf{x}_k| &= r_k(t_{ijk}). \end{aligned} \quad (10)$$

Solving for t_{ijk} we find

$$at_{ijk}^2 + bt_{ijk} + c = 0, \quad (11)$$

where

$$\begin{aligned} a &= 4v_b^2[v_b^2(\Delta \mathbf{x}_{ij}\Delta t_{ik} - \Delta \mathbf{x}_{ik}\Delta t_{ij})^2 - (\Delta \mathbf{x}_{ij} \times \Delta \mathbf{x}_{ik})^2], \\ b &= 4v_b^2\{v_b^2[\Delta \mathbf{x}_{ij} \cdot \Delta \mathbf{x}_{ik}\Delta t_{ij}\Delta t_{ik}(\Delta t_{ij} + \Delta t_{ik}) - \Delta \mathbf{x}_{ij}^2\Delta t_{ik}^3 - \Delta \mathbf{x}_{ik}^2\Delta t_{ij}^3] \\ &\quad + \Delta \mathbf{x}_{ij}^2\Delta \mathbf{x}_{ik}^2(\Delta t_{ij} + \Delta t_{ik}) - \Delta \mathbf{x}_{ij} \cdot \Delta \mathbf{x}_{ik}(\Delta \mathbf{x}_{ij}^2\Delta t_{ik} + \Delta \mathbf{x}_{ik}^2\Delta t_{ij})\}, \\ c &= v_b^4(\Delta \mathbf{x}_{ij}\Delta t_{ik}^2 - \Delta \mathbf{x}_{ik}\Delta t_{ij}^2)^2 + \Delta \mathbf{x}_{ij}^2\Delta \mathbf{x}_{ik}^2(\Delta \mathbf{x}_{ij} - \Delta \mathbf{x}_{ik})^2 \\ &\quad + 2v_b^2[(\Delta \mathbf{x}_{ij}^2\Delta t_{ik}^2 + \Delta \mathbf{x}_{ik}^2\Delta t_{ij}^2)\Delta \mathbf{x}_{ij} \cdot \Delta \mathbf{x}_{ik} - \Delta \mathbf{x}_{ij}^2\Delta \mathbf{x}_{ik}^2(\Delta t_{ij}^2 + \Delta t_{ik}^2)]. \end{aligned} \quad (12)$$

Any solution of this quadratic equation satisfying $t_{ijk} \geq t_k$ then corresponds to a potential defect formation event whose position is easily established using equation (4). The correct root is determined by checking for consistency with the appropriate equation (10). Rejecting any events occurring outside the simulation volume, the remaining 3-bubble collision events are stored in a time-ordered list.

B. Simulation

Having generated time-ordered lists of all 2-bubble collisions, potential fluxon releases, and 3-bubble collisions occurring within the simulation spacetime volume, we are now in a position to work through all these events incorporating them into the simulation in the correct time order. As we step through these events, however, we must also follow the motion of any free fluxons previously released from slow intersection points. At the time of its release a fluxon's velocity is in the direction of motion of the intersection point, and from equation (6) given by

$$\mathbf{v}_a = \frac{v_f}{|\mathbf{v}_{ij}|} \mathbf{v}_{ij}. \quad (13)$$

The free fluxon is then assumed to travel at a constant velocity until it hits a bubble wall, whereupon it undergoes a relativistic bounce (Fig. 4)

$$\begin{aligned} v_1 &= \frac{2v_b - (1 + v_b^2)u_1}{1 + v_b^2 - 2u_1v_b}, \\ v_2 &= u_2 \frac{1 - v_b^2}{1 + v_b^2 - 2u_1v_b}. \end{aligned} \quad (14)$$

Before including any event all the free fluxons in the simulation must be progressively updated to their positions at the time of the event. For each free fluxon $F_a \equiv (t_a, \mathbf{x}_a(t_a), \mathbf{v}_a(t_a))$ we calculate its collision time t_{aj} with bubble B_j from the condition

$$|\mathbf{x}_a(t_{aj}) - \mathbf{x}_j| = r_j(t_{aj}). \quad (15)$$

Solving for t_{aj} we find

$$at_{aj}^2 + bt_{aj} + c = 0, \quad (16)$$

where

$$\begin{aligned} a &= \mathbf{v}_a^2 - v_b^2, \\ b &= 2(\mathbf{x}_a - \mathbf{x}_j) \cdot \mathbf{v}_a - 2t_a \mathbf{v}_a^2 + 2t_j v_b^2, \\ c &= (\mathbf{x}_a - \mathbf{x}_j)^2 - 2t_a(\mathbf{x}_a - \mathbf{x}_j) \cdot \mathbf{v}_a + t_a^2 \mathbf{v}_a^2 - t_j^2 v_b^2, \end{aligned} \quad (17)$$

and reject as unphysical any roots which are imaginary or in the past ($t_{aj} < t_a$ or $t_{aj} < t_j$). Taking the smallest physical collision time the new fluxon position is simply

$$\mathbf{x}_a(t) = \mathbf{x}_a(t_a) + (t - t_a)\mathbf{v}_a(t), \quad (18)$$

and the new velocity given by equation (14). One further complication to note is that it is possible for a free fluxon to be re-captured by a fast intersection point; in this case we simply add the fluxon charge to whatever is already present at the intersection. This process is repeated until either the fluxon is re-captured or we reach the time of the event. Having thus updated every free fluxon we are now in a position to process the event itself.

If the event is a 2-bubble collision we first determine whether it closes off a region of false vacuum. This will only occur if the colliding bubbles are members of the same cluster. Thus if we assign each bubble a unique cluster number we can immediately tell whether a collision causes a closure or not. If the collision does not close, then we assign a fluxon–anti-fluxon pair at random to the two intersection points and re-number all the members of one cluster with the cluster number of the other. If the cluster does close, then we calculate the total charge within the closed region (from both fluxons trapped at intersection points and free fluxons now trapped inside the closed false vacuum region) and assign the fluxon–anti-fluxon pair so as to round the charge in the closed region to the nearest integer. If the closed region is bounded by three bubbles then, provided no bubble is nucleated within the region before it disappears, this integer charge will be that of the associated defect. Note that because of the possible presence of free fluxons the defect can have any integer charge, compared with the ± 1 charges possible in standard simulations.

If the event is a fluxon freeing, then we calculate its initial position and velocity as above and add it to the free fluxon list, ready for updating before the next event.

If the event is a 3-bubble collision, then we need to know if it is an external or an internal collision. If it is an external collision, then it will have been preceded by a closing 2-bubble collision and we will already know the charge associated with the defect. In this case we simply remove the associated fluxons from the simulation and add the defect position and charge to the defect list. For internal collisions free fluxons clearly play no role. We simply sum the fluxons at the two external intersection points and round the defect charge to the nearest integer. However in this case we also have to include the appropriate complementary fluxon at the emerging intersection point (Fig. 2b). If the emerging intersection point is slow then this fluxon is immediately freed as above. Furthermore the convergence of the two external intersection points may reduce a closed region bounded by four bubbles to one bounded by three, in which case the new bounded charge should be calculated ready for the ensuing external 3-bubble collision.

It should be noted that at various points during these calculation it is necessary to test two real numbers for equality. Since this can only be done to finite accuracy we have to include a difference cutoff, below which two numbers are deemed to be equal. To the extent that this introduces a minimal measureable space and time interval there is still some discretization inherent in these simulations.

A few snapshots of the simulation for the case $v_b/v_f = 0.5$, with the resulting system of vortices, are shown in Fig. 5. The vortex distributions obtained for $v_b/v_f = 1$ and using the standard lattice simulation of defect formation [6] are shown in Fig. 6 for comparison.

IV. RESULTS

We are interested in the variation in the defect statistics with the ratio v_b/v_f . For each value of this ratio, we must nucleate a sufficient number of bubbles to fill the simulation

space by the end of the simulation time. However we can then draw the statistics of interest only from the region sufficiently far away from the edge of the simulation not to have been affected by the absence of bubbles beyond the edge. Since the fluxons are taken to have $v_f = 1$, for a 2+1 dimensional simulation of size X^2 and duration T this region covers the range $(T, X - T)$ in each direction. To obtain reasonable statistics we ensure that this ‘safe’ region contains of the order of 100 bubbles and then calculate

1. the ratio of the number of defects to the number of bubbles, N_d/N_b .
2. the ratio of the mean minimum defect–anti-defect separation to the mean minimum defect–defect separation, $R \equiv \langle D_{d\bar{d}} \rangle / \langle D_{dd} \rangle$.
3. the fraction of the defects of charge $|Q| = n$ for $n = 1, 2, \dots$

The smaller v_b is the more bubbles we need to fill the simulation volume whilst generating 100 ‘safe’ bubbles, and we are constrained by computing resources to $v_b/v_f \geq 0.2$. The results, averaged over 100 runs for each value of v_b/v_f , are shown in Fig. 7.

V. DISCUSSION

Our goal in this paper was to study the statistical properties of the system of vortices formed in a first-order phase transition. In particular, we were interested in the dependence of these properties on the speed of bubble expansion, which is characterized in our model by the parameter v_b/v_f . Our main results are presented in Fig. 7 which shows the number of vortices formed per bubble and the ratio of the average nearest-neighbor vortex–anti-vortex and vortex–vortex distances, $R = \langle D_{d\bar{d}} \rangle / \langle D_{dd} \rangle$, as functions of v_b/v_f . The ratio R gives a quantitative measure of the vortex–anti-vortex correlation.

We see, first of all, that the number of vortices decreases as v_b gets smaller (at fixed v_f). This is not difficult to understand. At low values of v_b , fluxon escape prevents the formation of vortices in places where they would otherwise be formed. The escaped fluxons are eventually captured, but they mix with the escaped anti-fluxons, and there is a tendency for the net flux to cancel. Annihilation of large groups of fluxons and anti-fluxons can be seen in Fig. 5.

Apart from a decrease in the number of defects, a visual inspection of vortex distributions in Figs. 5e and 6a suggests that the flux escape decreases correlation between vortices and anti-vortices. For $v_b = v_f$ there is no flux escape, and the distribution in Fig. 6a contains many close vortex–anti-vortex pairs, while there are very few such pairs for $v_b = 0.5v_f$. This trend is confirmed by the graph in Fig. 7 which shows a decrease in vortex–anti-vortex correlation with a decreasing speed of bubble walls v_b .

It is interesting to compare the vortex distribution for $v_b = v_f$ with that obtained using a random-phase lattice simulation (Fig. 6b). The visual appearance of the latter distribution is quite different, but it also shows a strong correlation between vortices and anti-vortices. The nearest neighbors of almost all vortices are anti-vortices and vice versa. A calculation of the ratio R for the lattice simulation gives $R = 0.58$, which is fairly close to the value $R = 0.5$ for $v_b = v_f$. The difference probably arises from the fact that the lattice imposes a minimum defect–anti-defect separation distance. It is noteworthy that R decreases with

decreasing defect density. This is in contrast to the ‘biased’ case when the order parameter potential is tilted [8]. There it is found that R decreases with increasing defect density.

The strong vortex–anti-vortex correlation in lattice simulations has been known for a long time [9]. The total magnetic flux Φ through a region of size L is proportional to the phase variation around the region’s perimeter. If the phase varies at random on the scale of the lattice spacing ξ , we have $\Phi \propto (L/\xi)^{1/2}$. On the other hand, the number of defects inside the region is $N \sim (L/\xi)^2$, and an uncorrelated distribution would give a much larger flux, $\Phi \propto N^{1/2} \sim L/\xi$. Essentially the same argument applies to our bubble simulation, but now the spread in bubble sizes results in a spread in the nearest-neighbor separations. This spread is responsible for the different visual appearance of the two distributions.

The decrease in the vortex–anti-vortex correlation at low bubble speeds can be easily understood. Correlations are destroyed when fluxons escape from the bubble intersections where they originated. The escaped fluxons form a random gas, and we expect no correlations on small scales, where fluxons and anti-fluxons had enough time to randomize. If L_r is the characteristic scale on which randomization has occurred, then we expect magnetic flux fluctuations to scale as $\Phi \propto N^{1/2}$ for $L < L_r$ and as $\Phi \propto N^{1/4}$ for $L > L_r$.

We finally briefly discuss the implications of our results for defect formation in three-dimensional phase transitions. As already mentioned in the Introduction, a close vortex–anti-vortex pair is a two-dimensional analogue of a small closed loop of string. Our results suggest that magnetic flux spreading will decrease the amount of string in small loops relative to the infinite strings.

If magnetic monopoles are formed in a slow first order phase transition, we expect a decrease in the monopole density and in the correlation between monopoles (M) and anti-monopoles (\bar{M}). For a suitably defined scale L_r , the magnetic charge fluctuations will scale as $N^{1/2}$ for $L < L_r$ and as $N^{1/3}$ for $L > L_r$. This randomization of the monopole distribution can be important in models where monopoles get connected by strings, particularly in Langacker-Pi-type models [10] where strings disappear at a subsequent phase transition. If M ’s and \bar{M} ’s are strongly correlated, as in second-order or fast first-order transitions, then most of the $M\bar{M}$ pairs get connected by the shortest possible strings of length l comparable to the average inter-monopole distance d . Longer strings with $l \gg d$ are exponentially suppressed [11], [12]. For monopoles formed in a slow first-order transition, the length distribution of strings can be much broader. Since the lifetime of $M\bar{M}$ pairs is determined mainly by the time it takes to dissipate the energy of the string, the number of monopoles surviving after the strings disappear can be significantly affected.

ACKNOWLEDGMENTS

We are indebted for hospitality to the Isaac Newton Institute for Mathematical Sciences, Cambridge, England, where this work was initiated. The work of AV was supported in part by the National Science Foundation. TV wishes to thank the Rosenbaum Foundation for the award of a Fellowship at the Isaac Newton Institute.

REFERENCES

- [1] For recent reviews, see A. Vilenkin and E.P.S. Shellard, *Cosmic Strings and other Topological Defects* (Cambridge University Press, Cambridge, 1994); M.B. Hindmarsh and T.W.B. Kibble, *Cosmic Strings*, to be published in Rep. Prog. Phys. (hep-ph/9411342).
- [2] S. Rudaz and A.M. Srivastava, Mod. Phys. Lett. **A8**, 1443 (1993).
- [3] M. Hindmarsh, A.-C. Davis and R. Brandenberger, Phys. Rev. **D49**, 1944 (1994).
- [4] T.W.B. Kibble, J. Phys. A: Math. & Gen. **9**, 1387 (1976).
- [5] T.W.B. Kibble and A. Vilenkin, “Density of strings formed at a second-order cosmological phase transition”, submitted to Phys. Rev. Letters (hep-ph/9501207).
- [6] T. Vachaspati and A. Vilenkin, Phys. Rev. **D30**, 2036 (1984).
- [7] T.W.B. Kibble and A. Vilenkin, “Phase equilibration in bubble collisions”, submitted to Phys. Rev. D (hep-ph/9501266).
- [8] T. Vachaspati, Phys. Rev. **D44**, 3723 (1991).
- [9] M.B. Einhorn, D.L. Stein and D. Toussaint, Phys. Rev. **D21**, 3295 (1980).
- [10] P. Langacker and S.-Y. Pi. Phys. Rev. Lett. **45**, 1 (1980)
- [11] P. Sikivie, in Proceedings of the Summer School on Particle Physics, Gif-sur-Yvette (1983)
- [12] E.J. Copeland, D. Haws, T.W.B. Kibble, D. Mitchell and N. Turok, Nucl.Phys. **B298**, 445 (1986)

FIGURES

FIG. 1.

An ‘external’ collision of three bubbles (a) before the collision, (b) at the collision, showing the formation of a vortex. In all such figures squares represent fluxons and circles vortices, with black being positively and white negatively charged.

FIG. 2.

An ‘internal’ collision of three bubbles (a) before the collision, (b) at the collision, showing the formation of a vortex and a compensating anti-fluxon.

FIG. 3.

The geometry of a two-bubble collision.

FIG. 4.

The relativistic bounce of a fluxon off a bubble.

FIG. 5.

Snapshots of the simulation at six equally spaced times (a)–(f) for the case $v_b/v_f = 0.5$.

FIG. 6.

The final vortex distributions obtained (a) for $v_b/v_f = 1$ and (b) from the standard Vachaspati-Vilenkin lattice simulation for comparison.

FIG. 7.

The mean number of defects per bubble (circles) and the ratio between the mean nearest-neighbour defect–anti-defect and defect–defect distances (squares) plotted against the velocity ratio v_b/v_f . The error bars indicate standard deviations over 100 runs.

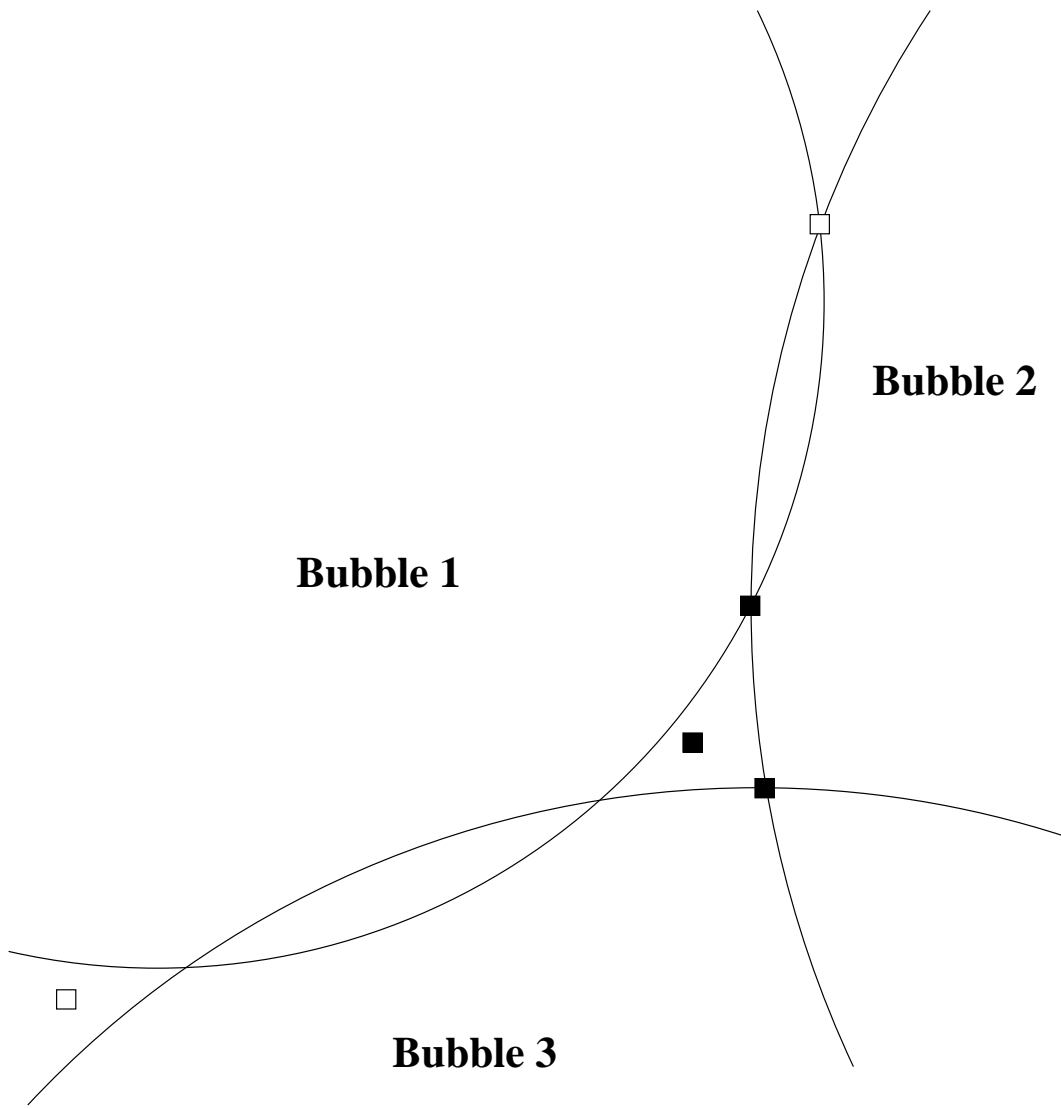


Figure 1 (a)

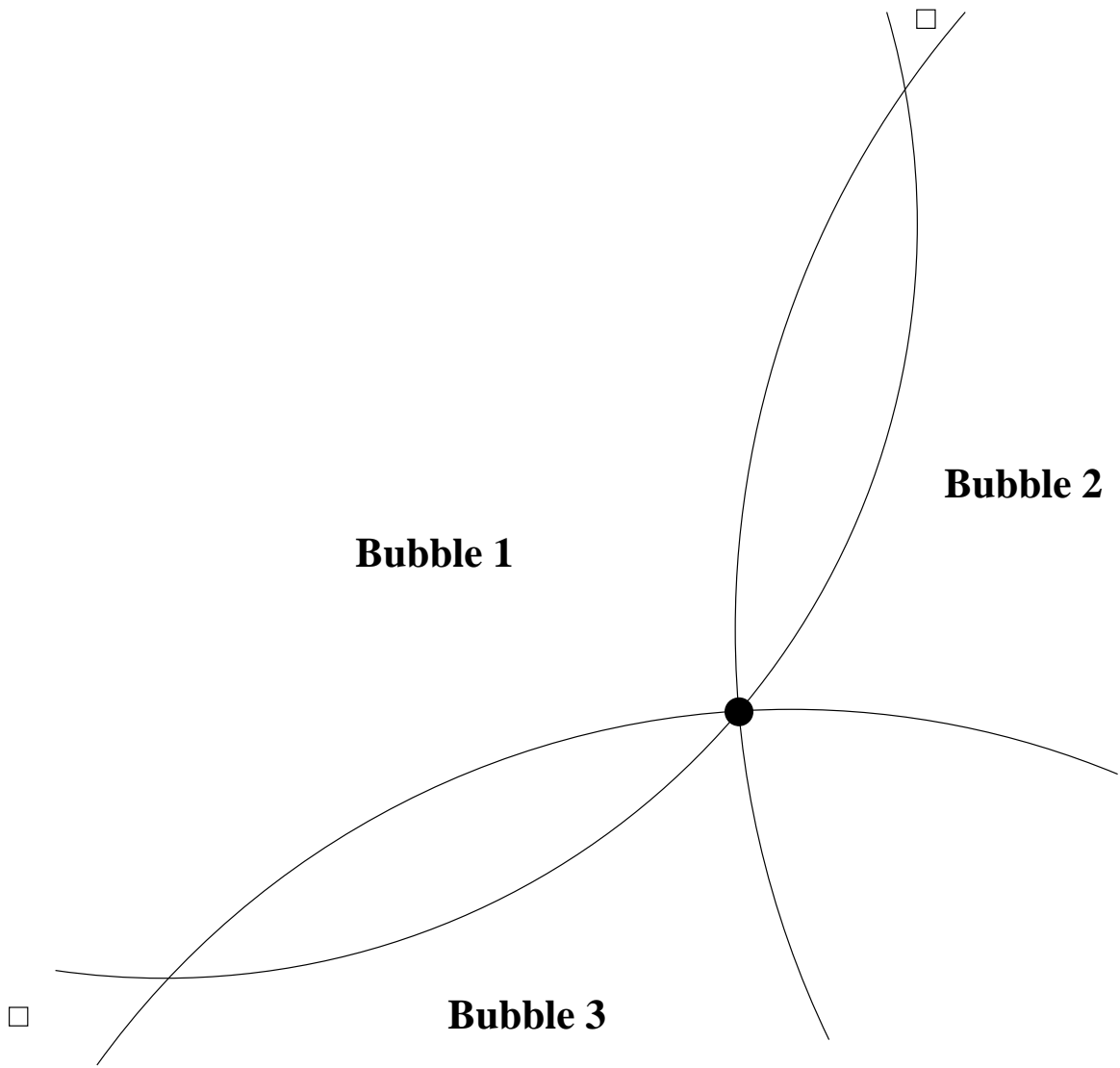


Figure 1 (b)

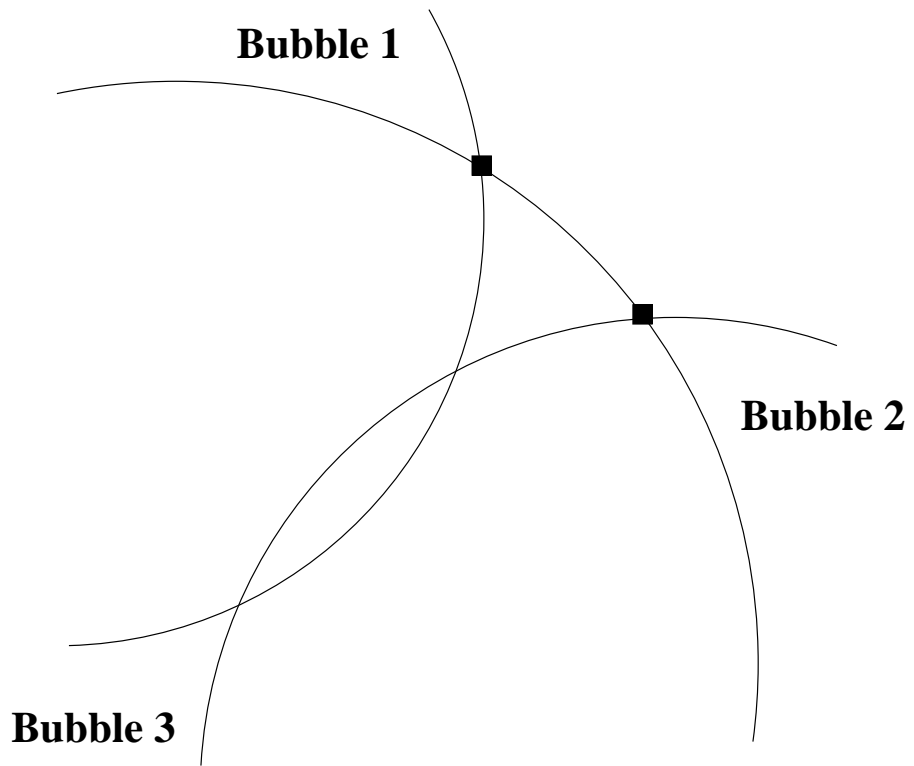


Figure 2 (a)

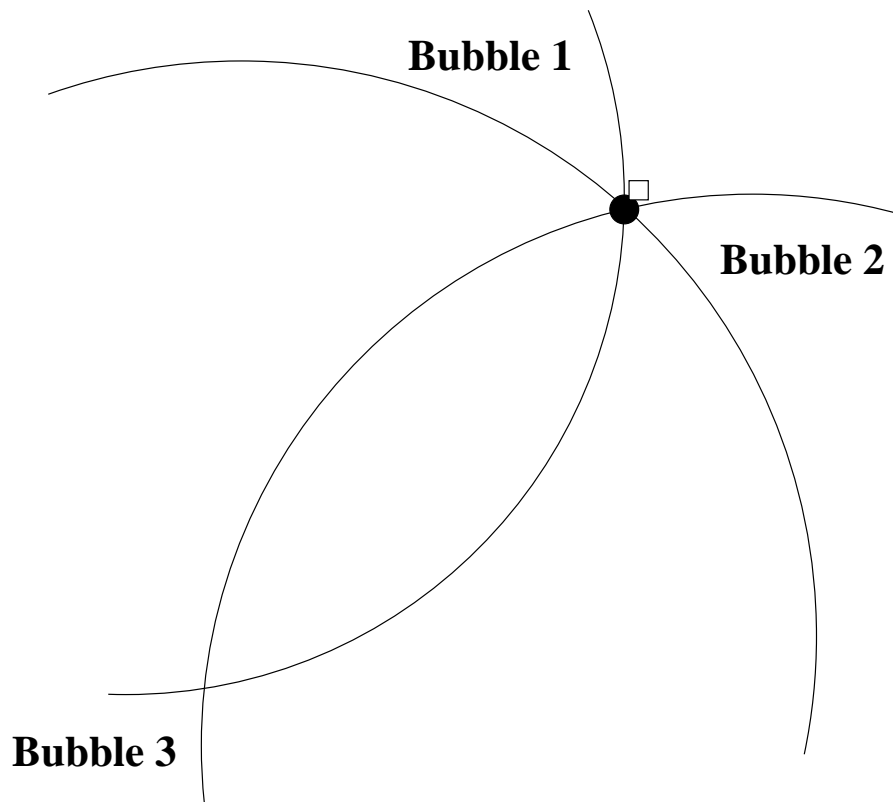


Figure 2 (b)

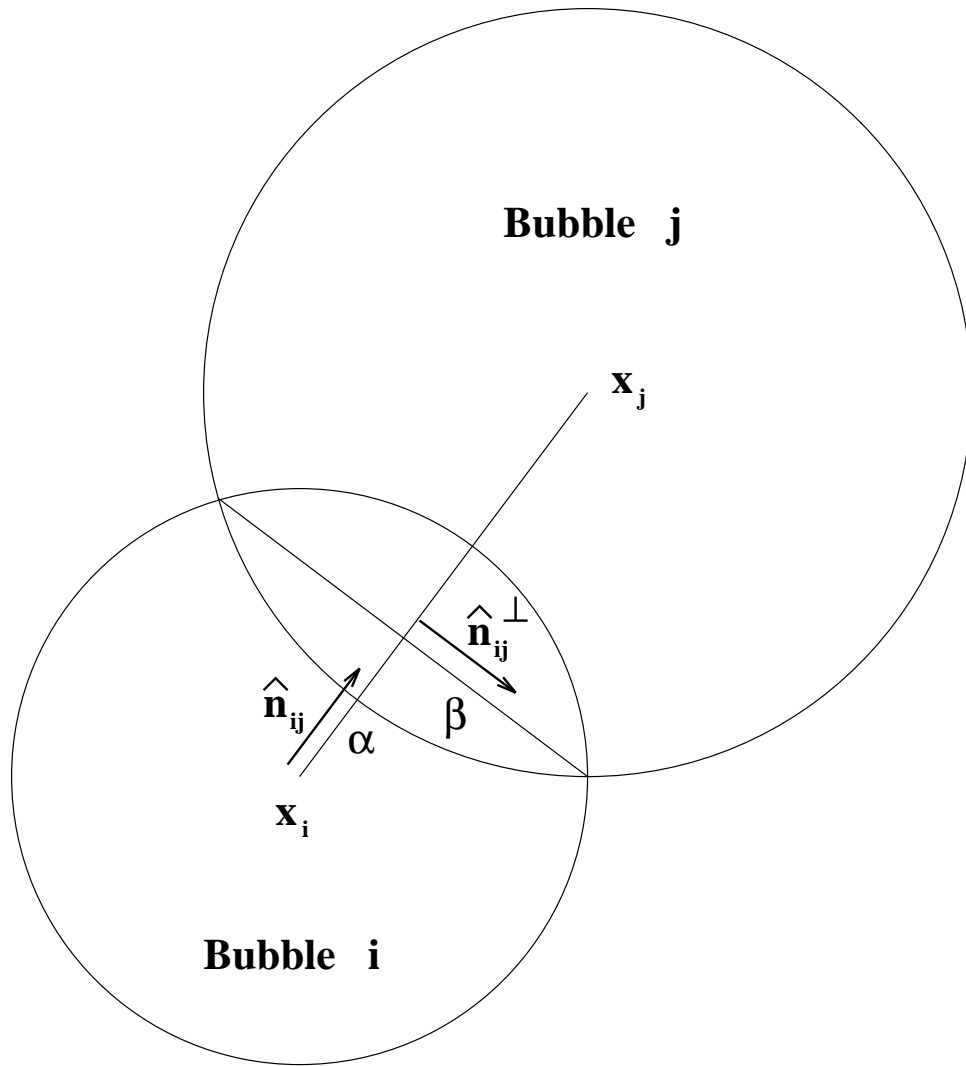


Figure 3

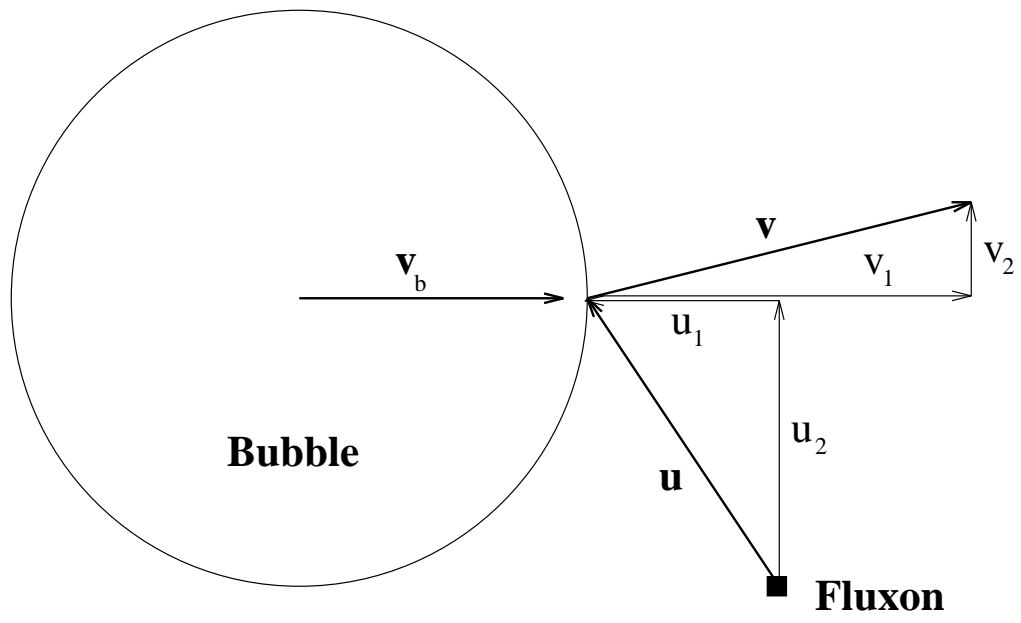


Figure 4

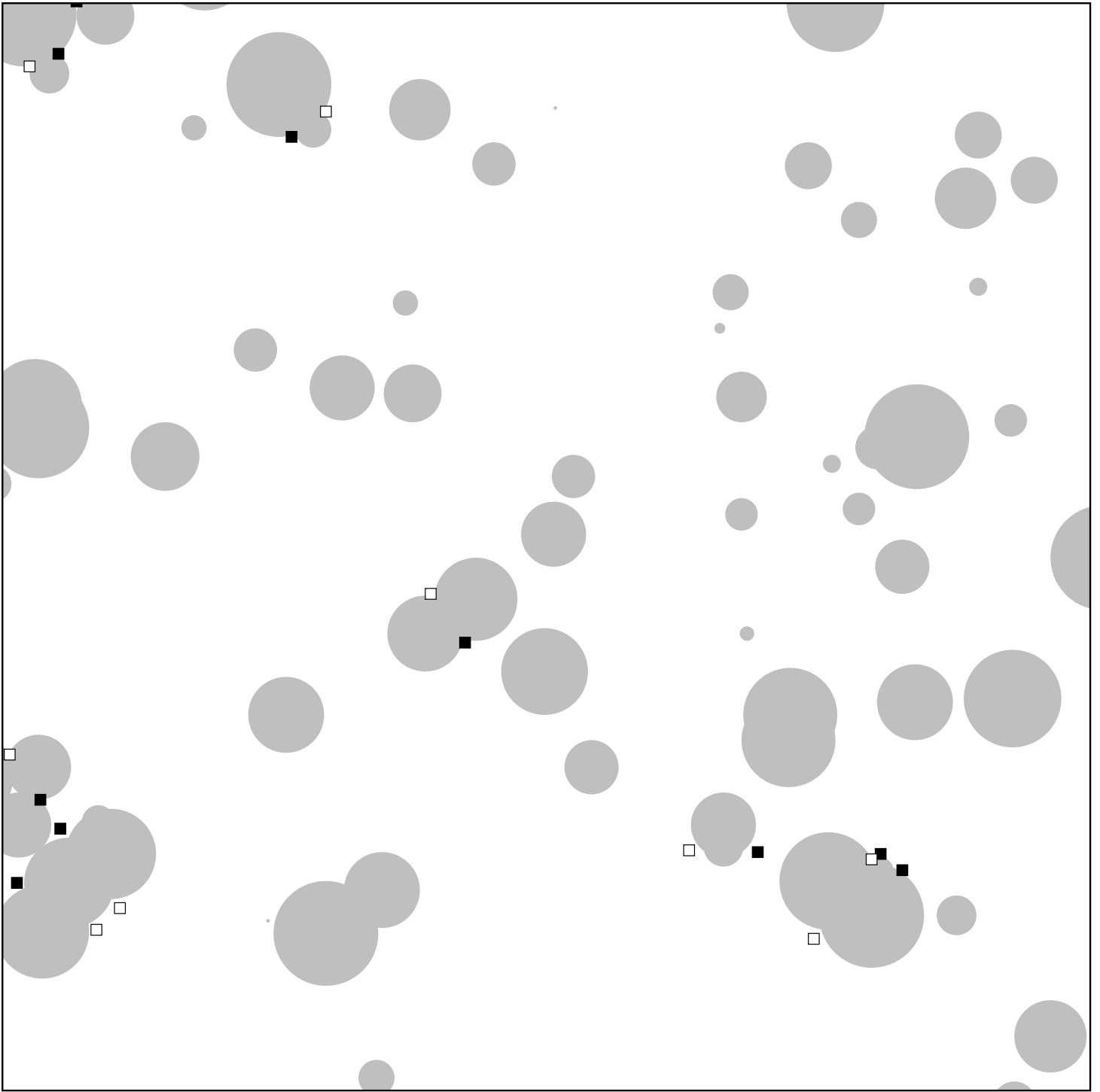


Figure 5 (a)

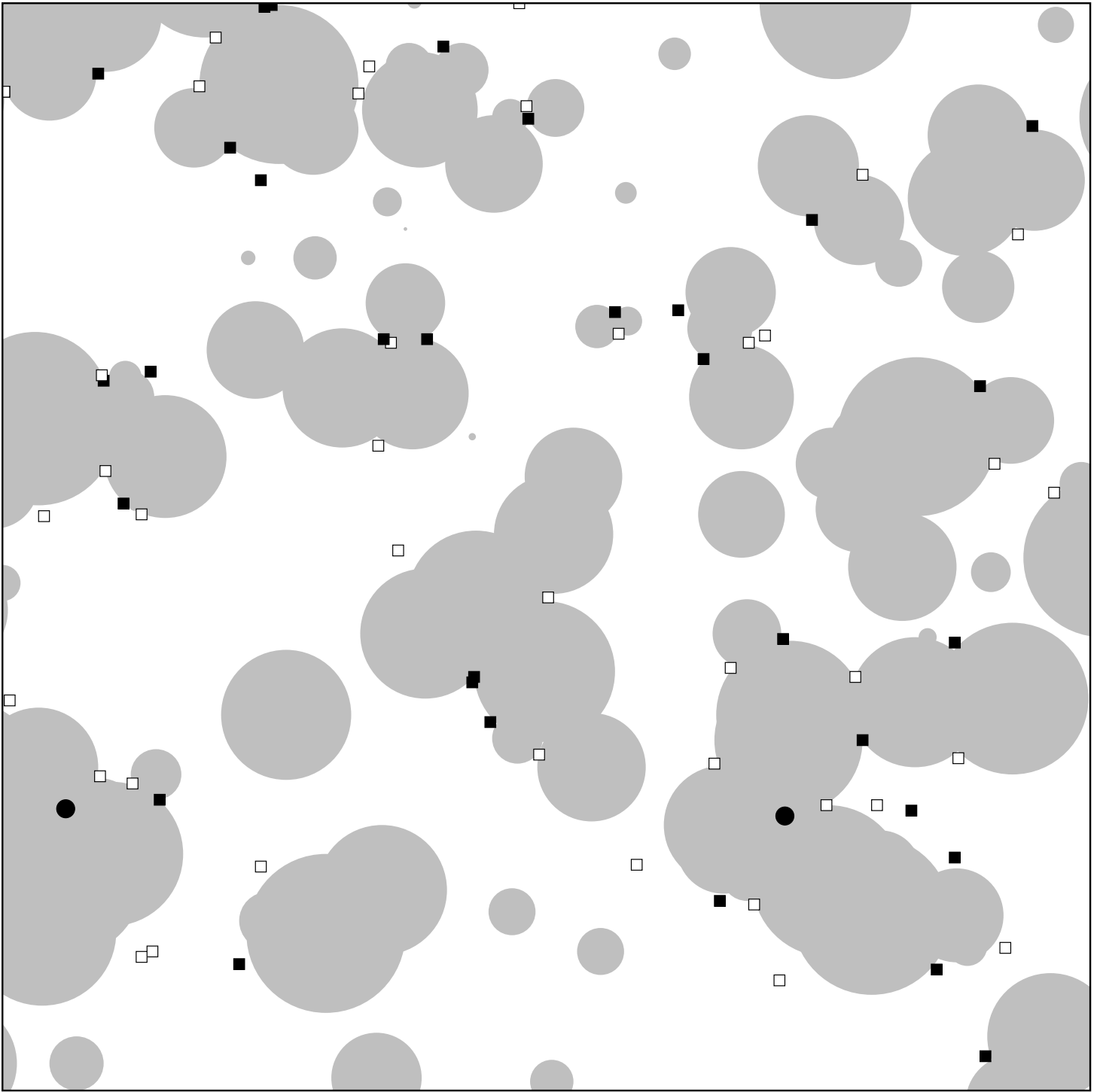


Figure 5 (b)

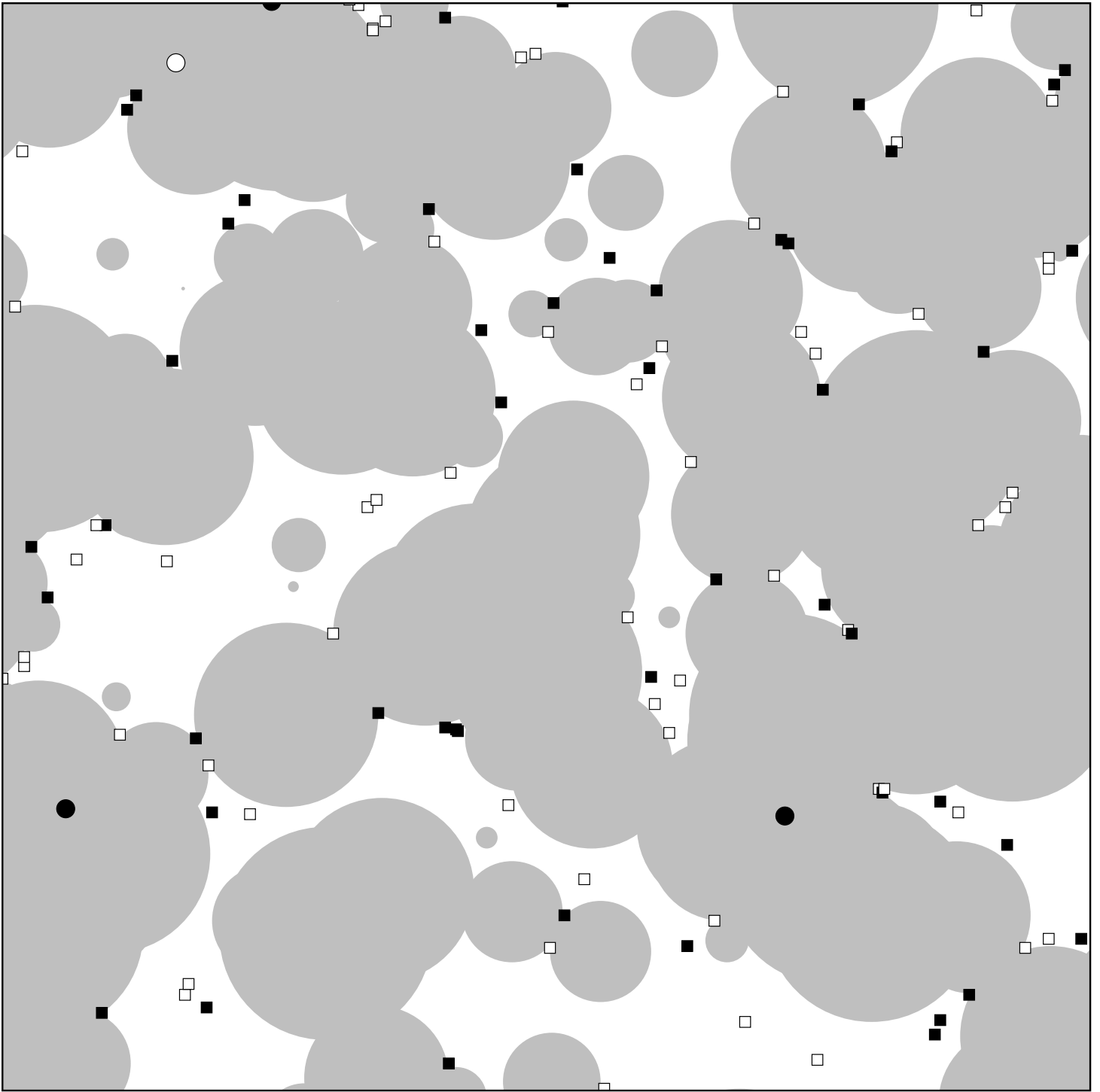


Figure 5 (c)

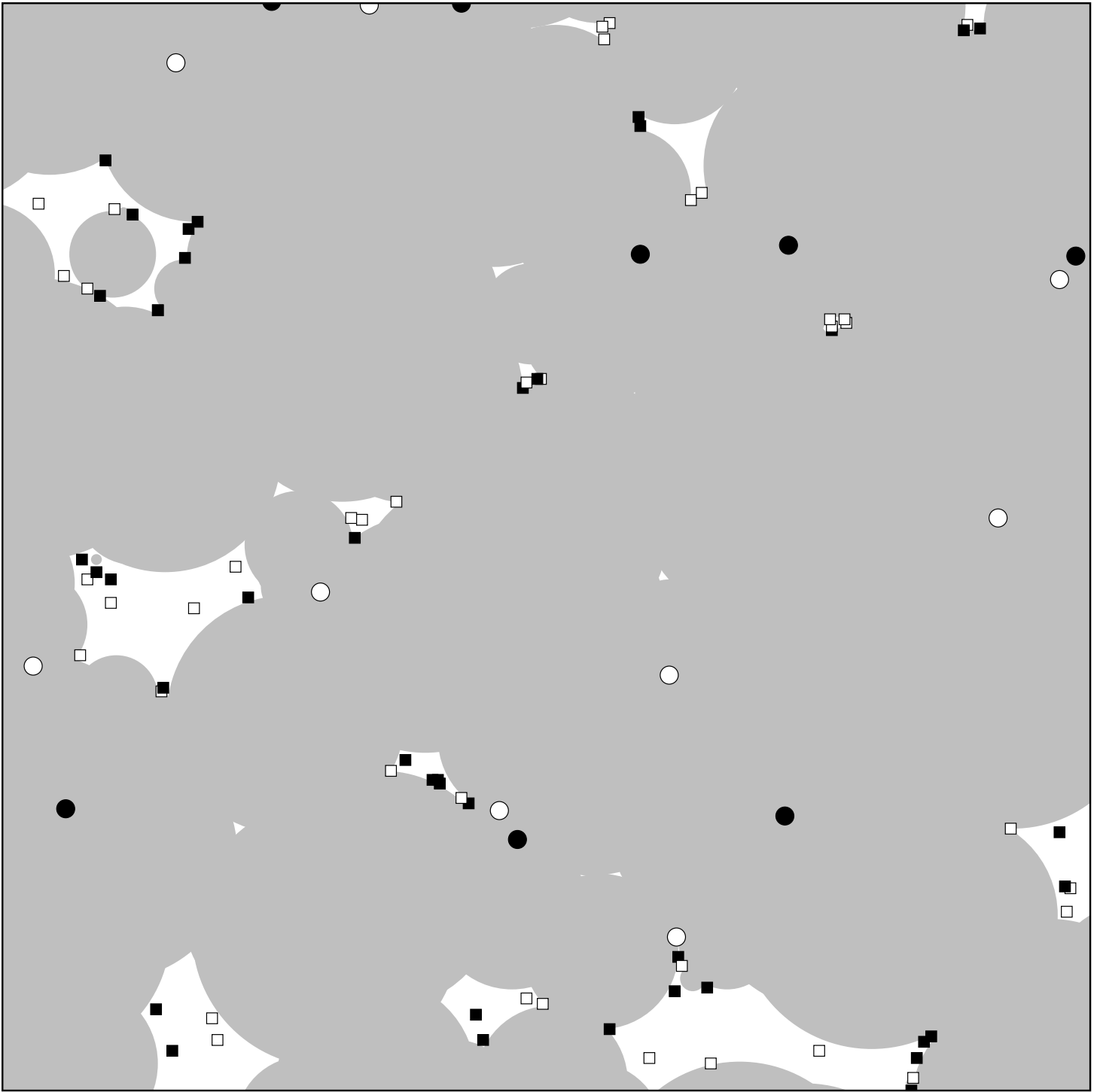


Figure 5 (d)

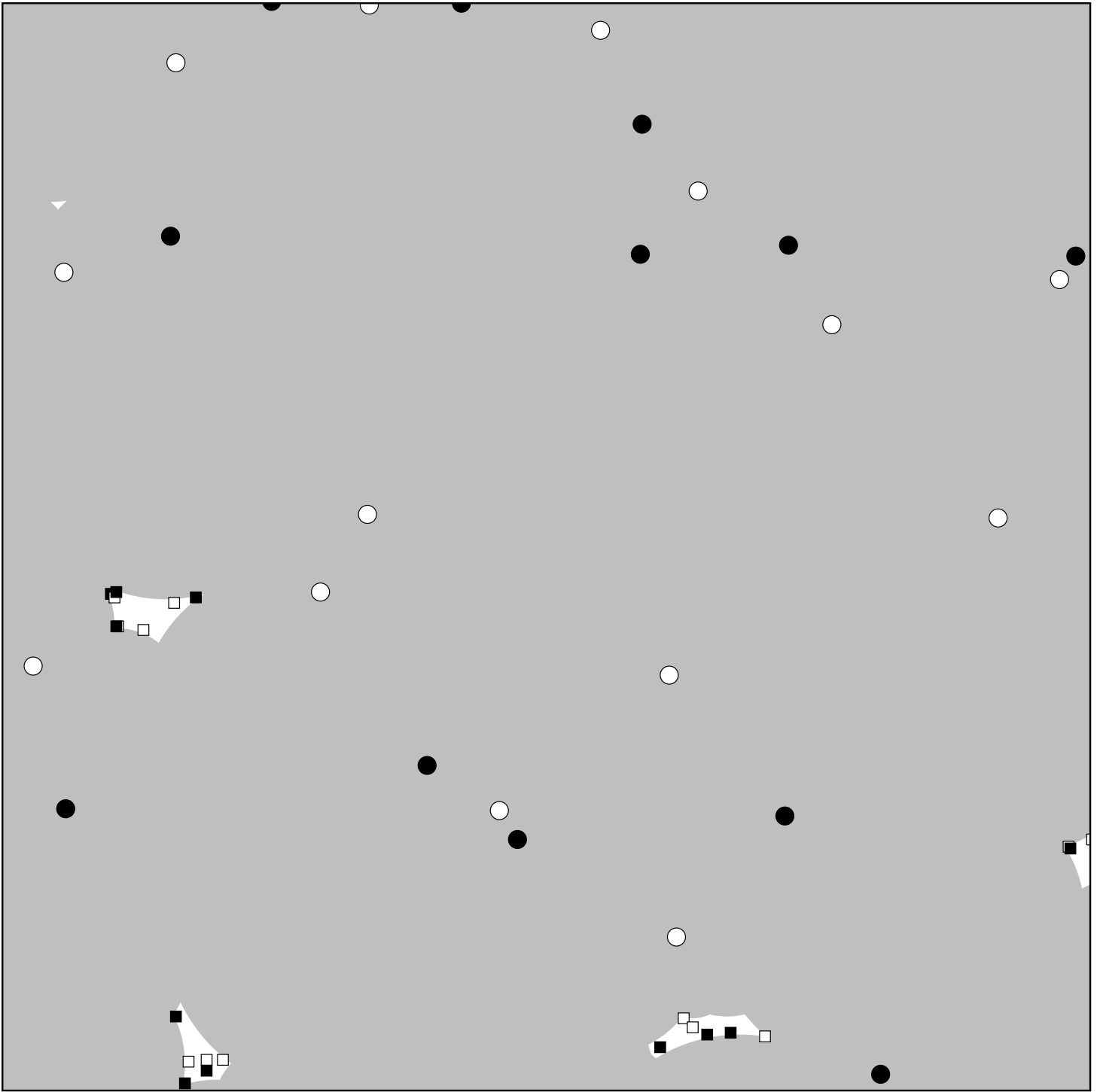


Figure 5 (e)

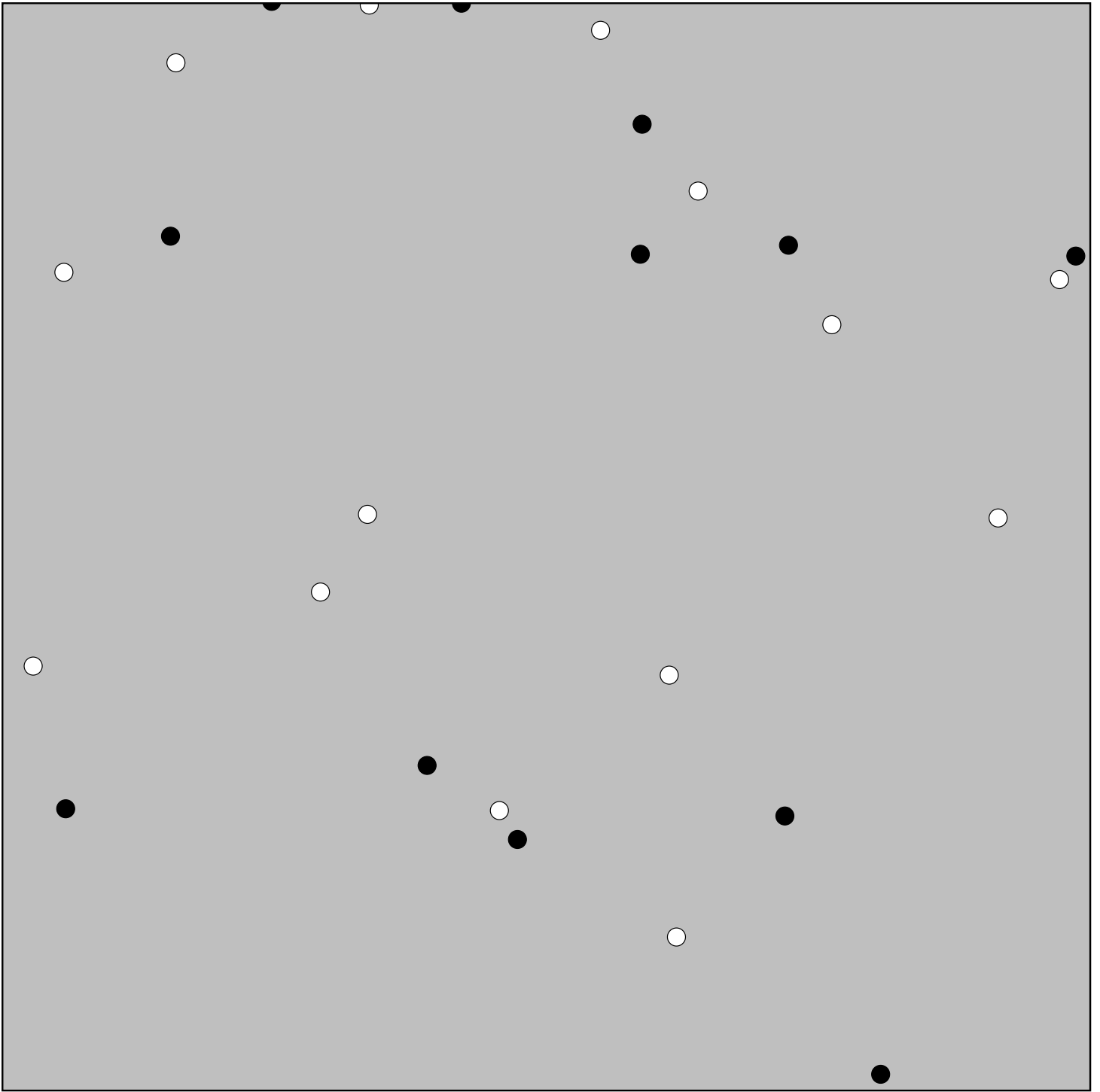


Figure 5 (f)

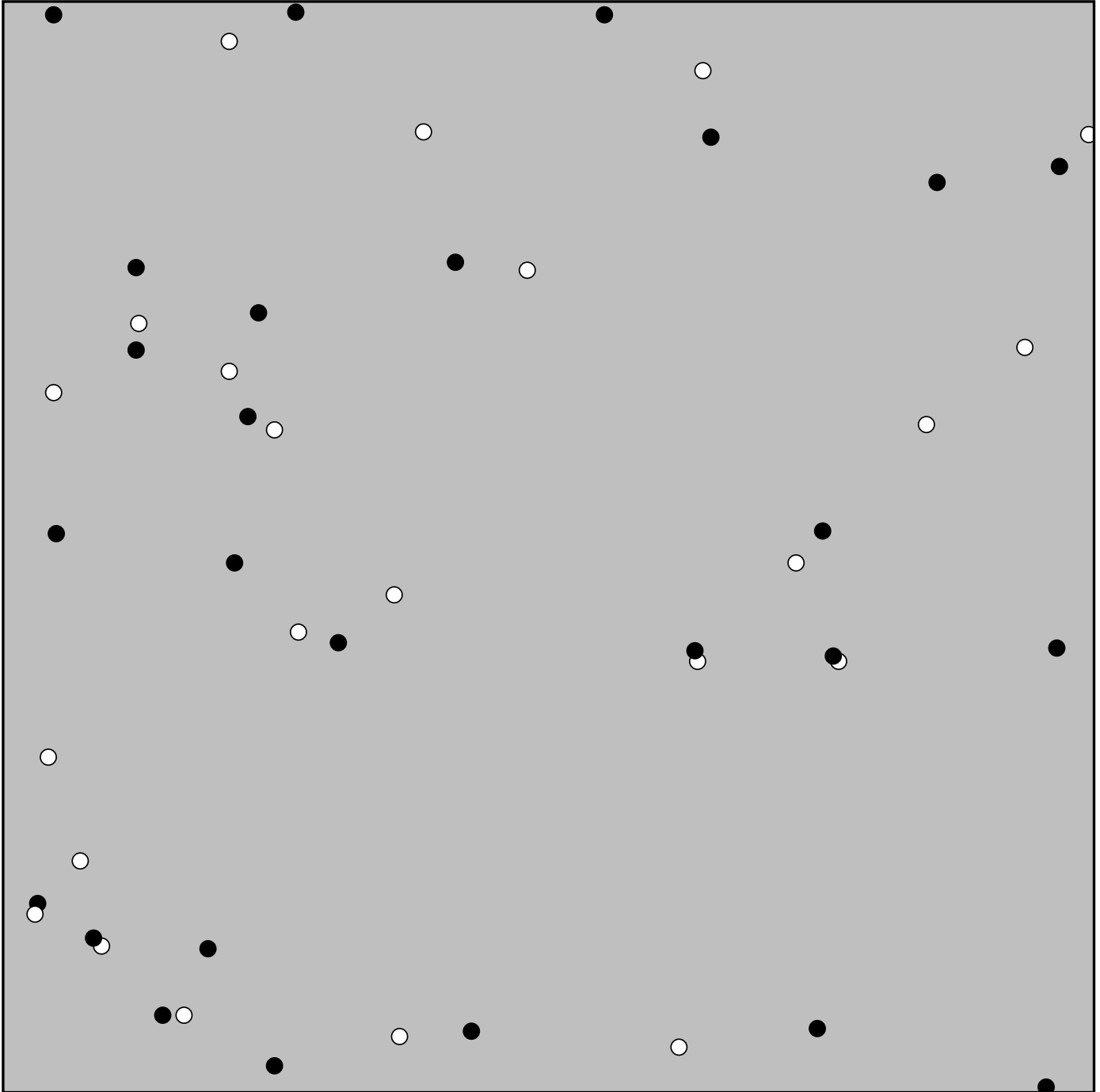


Figure 6 (a)

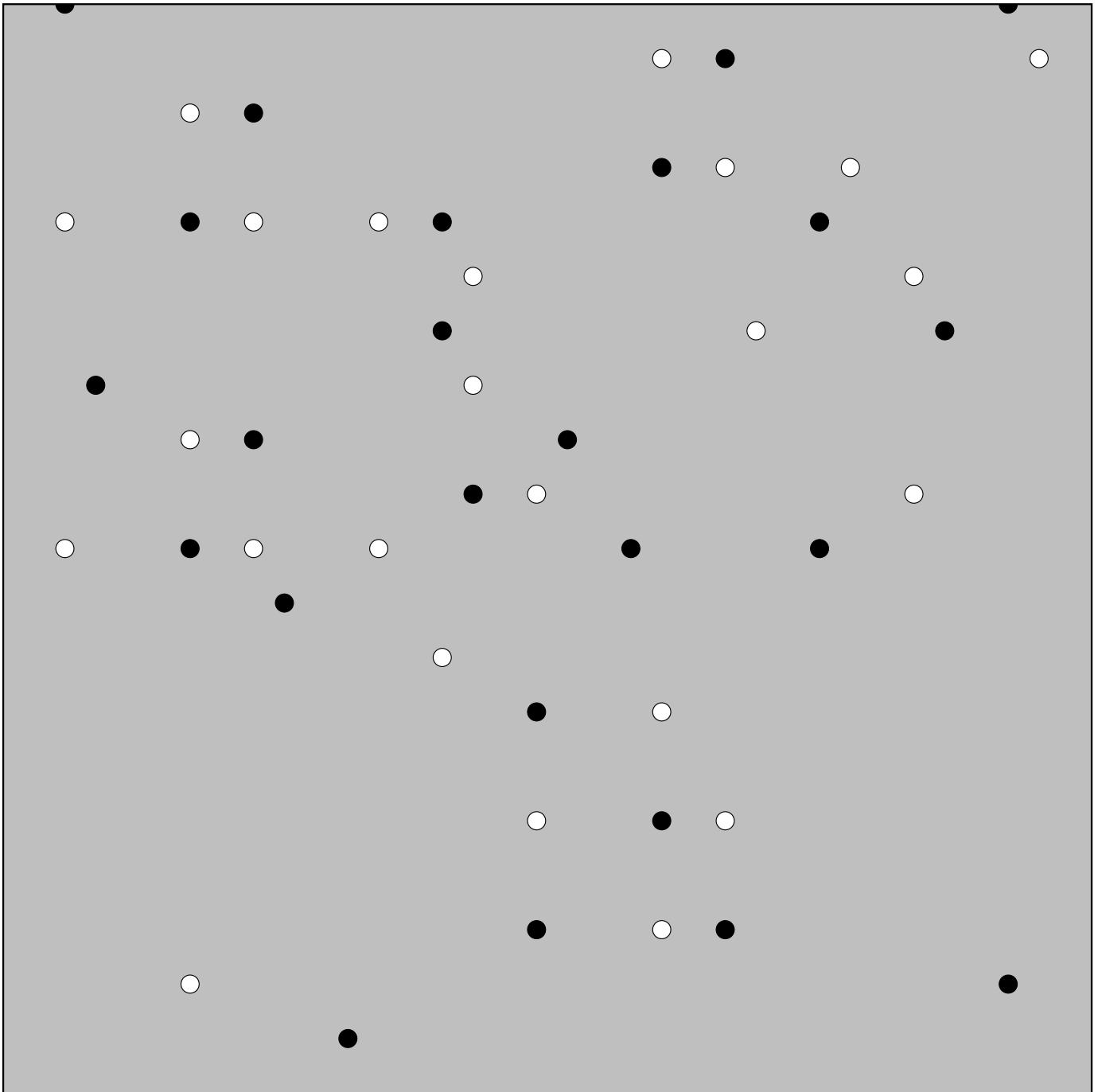


Figure 6 (b)

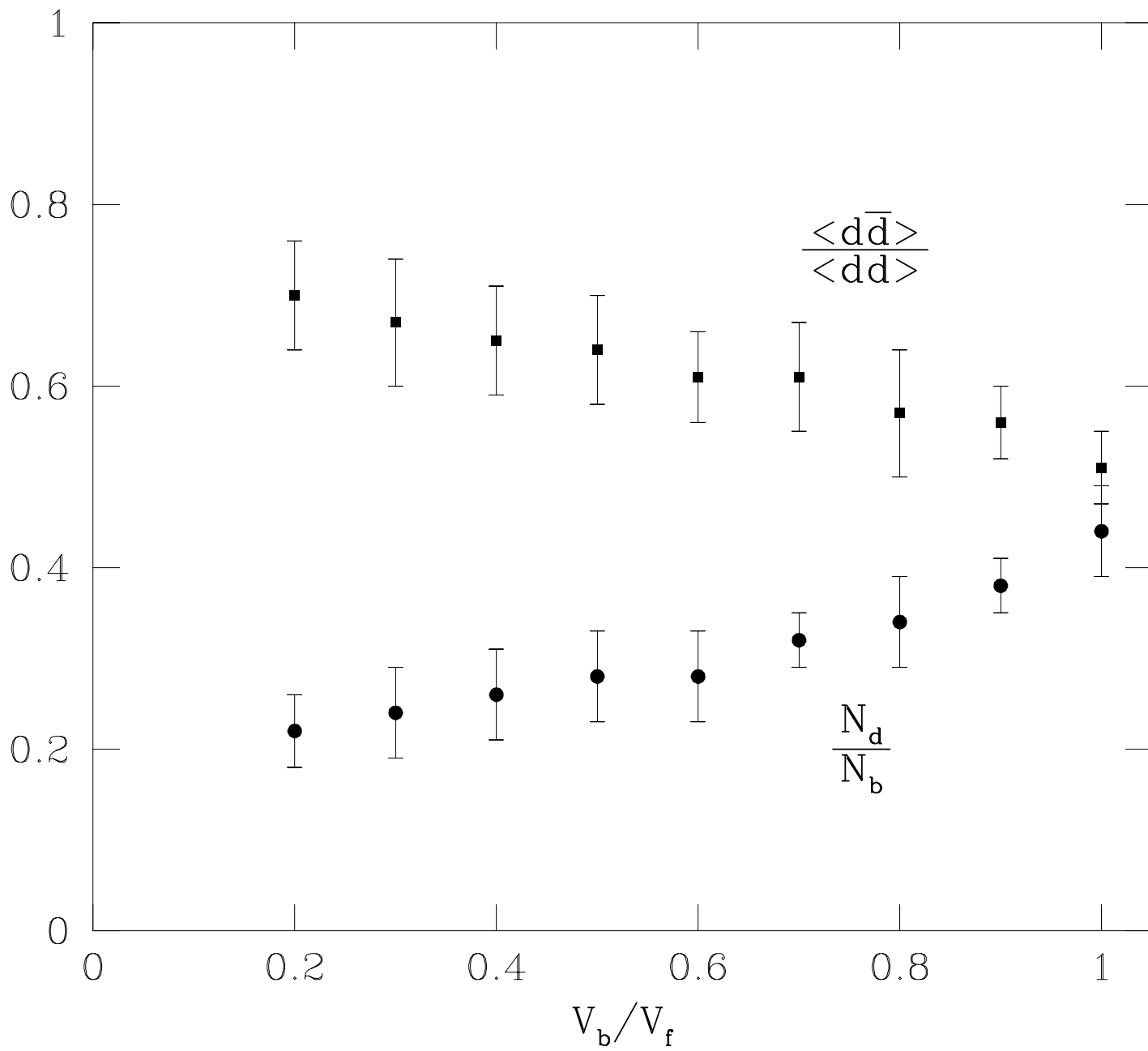


Figure 7